International Journal of Minerals, Metallurgy and Materials https://doi.org/10.1007/s12613-020-2046-8

International Journal of Minerals, Metallurgy and Materials
Accepted manuscript, https://doi.org/10.1007/s12613-020-2046-8

The investigation of wear and mechanical properties of carburized AISI 8620 steel by powder metallurgy

Mehmet Akif Erden[1)] *and Fatih Aydin*[2)]
1) Department of Biomedical Engineering, Karabuk University, Karabuk 78050, Turkey
2) Department of Metallurgical and Materials Engineering, Karabuk University, Karabuk 78050, Turkey

Corresponding author: Fatih Aydin E-mail: fatih.aydin@karabuk.edu.tr

Abstract

In this study, the effect of carburizing on tensile strength and wear resistance of AISI 8620 steel were investigated. Firstly, the alloy with 0.25 %C content was pressed at 700 MPa and sintered at the temperature of 1300°C, 1400°C and 1500°C for 1 hr. After determination of ideal sintering temperature, the carburizing process was applied to Alloy 1 and Alloy 2 (0.2 C% and 0.25%C) at 925°C for 4 h. The microstructure of the samples was characterized by Optical microscopy(OM), scanning electron microscopy (SEM). The mechanical and wear behavior of carburized and non-carburized samples were investigated by hardness, tensile and wear tests. The increase in ultimate tensile strength for Alloy 1 and Alloy 2 after carburizing was calculated as 134.4% and 138.1%, respectively.However, the decrease in elongation % for Alloy 1 and Alloy 2 after carburizing was determined as 62.6 % and 64.7 %, respectively. It is reported that the wear depth values of Alloy 2 for non-carburized and carburized conditions under load of 30 N is 231.2 µm and 100.1 µm, respectively. It is observed that oxidative wear changed to abrasive wear for the transition from load of 15N to load of 30N for Alloy 1 and Alloy 2.

Keywords: powder metallurgy; carburizing PM steels; microstructure; wear; mechanical properties

1. Introduction

Steels are manufactured in different specifications according to the purpose of use of the industry [1-5]. The mechanical properties of the steels vary considerably depending on the alloying elements, microstructure, grain sizes and the heat treatments applied [6]. To this end, steel is subjected to many heat treatment applications such as carburizing, normalization, annealing, austempering, martempering and boronizing. It is well known that carburizing is one of the most important surface hardening process. At the end of the process, the surface of the part is hard and resistant to abrasion, while the core part is soft with respect to the surface [7].

In the literature, there are several studies on carburizing treatment applied to AISI 8620 steel and low alloy steels produced by casting. Tabur et al. examined the tribological performance of gas carburized AISI 8620 steel (925 °C-5.3hr and 11hr) for different case depth. It was concluded that carburizing time significantly affects the case depth. It is also reported that higher case depth leads to increase in wear resistance [8]. Erdogan et al. studied the carburizing of the dual-phase AISI 8620 steel (925°C-11hr) and investigated the effect of martensite volume fraction (MVF) and martensite particle size (MPF) on tensile properties. The best mechanical property of the sample was reported for fine MPS at a MVF of 25% [9]. Özbek et al. have studied the hardness and wear behavior of AISI 8620 steel carburized for 1 hr at 900°C by pulse-plasma treatment. It was reported that the pulse-plasma treatment leads to increase in wear performance [10].

Patidar et al. studied the carburized mild steel at 950 °C with soaking time of 2 hr and then tempered with different temperature range for different soaking time. The mechanical and wear tests were conducted for the samples. It was reported that tribological performance and mechanical properties improved with increasing tempering temperature [11]. Kumar et al. have studied the abrasive wear characteristics of carburized low carbon steels, heat treated medium carbon and alloyed steels. It was found that the abrasion resistance of carburized steels increased with increasing carburization temperature [12]. Panda et al. have investigated the mechanical and wear behaviour of carburized low carbon steels. The samples were carburized at the temperature of 850ºC, 900 ºC and 950 ºC. The best mechanical and wear properties was obtained for the sample that carburized at the temperature of 950 ºC [13]. Abdulrazzaq examined the hardness and wear behaviour of carburized low carbon steel in oil media. The sample was carburized at 950 ˚C for 2 hr, 4 hr and 6 hr. It was reported that as carburizing temperature increases, wear resistance of the samples increased [14]. Elzanaty investigated the carburization on the mechanical properties of mild steel. The samples were carburized at temperature range of 850 ^{o}C to 950 ^{o}C. After that the samples were tempered at 200^{o}C for 30 min. The results showed that increasing carburization temperature give rise to significant improvement in mechanical properties [15].

Powder metallurgy has several advantages compared to other production methods. It is economically feasible to produce the high-precision parts with high precision. In powder metallurgy, some process steps are not applied, so it is possible to manufacture parts which are suitable for direct usage [16].

It is understood that no study was present on carburizing treatment applied to AISI 8620 steel produced by powder metallurgy. However, there are several studies on the effect of carburizing process on mechanical properties of steels with different chemical compositions produced by powder metallurgy. Emamian has examined the wear and impact behaviour of carburized low alloy steels produced by powder metallurgy. It is pointed out that surface treatments increase the wear performance of P/M parts for service conditions [17]. Dong et al. have examined the microstructure of P/M steels via carbusintering process. The influence of sintering parameters was studied. The hardness and impact energy were improved to 484 HV and 13 J, respectively [18]. Georgiev et al. have studied the wear behaviour of carburized Fe-3Mn-0.8C steel produced by powder metallurgy and reported that carburizing leads to significant increase in wear resistance for sintered gear wheels [19].

In this study, firstly, AISI 8620 steel with 0.25 C% content was produced by powder metallurgy and different sintering temperatures (1300°C, 1400 °C and 1500°C) were applied for 1 h. After the determination of optimum sintering condition, two different steels (0.2%C and 0.25 %C content) were produced and carburized at the temperature of 925 °C for 4 h. The hardness, microstructure, tensile and wear behaviour of the samples were investigated in detail.

2. Experimental study

The properties of powders for the production of AISI 8620 steels were given in Table 1.

Table 1. The properties of the powders.

Elemental Powders	Size / μm	Purity / %
Iron (Fe)	<150	99.9
Graphite	10–20	96.5
Chromium (Cr)	≤44	99
Molybdenum (Mo)	≤150	99.9
Nickel (Ni)	≤5	99.7

So as to manufacture the AISI 8620 steel, the powders were mixed using TURBULA T2F mixer for 2 hr. Firstly, the production of Alloy 2 was performed. The mixed powders were pressed as a tensile test specimen according to ASTM E8/E8M with 700 MPa in a hydraulic press (Hidroliksan). The pressed samples was sintered at 1300°C, 1400°C and 1500°C under argon environment. The sintering temperature was kept as 1 hr. Three samples were manufactured for each composition. The chemical composition of steels was given in Table 2.

Table 2. The chemical composition of alloys for this study (wt%) .

Materials	Graphite	Cr	Mo	Ni	Fe
Alloy 1	0.2	0.45	0.15	0.4	Rest.
Alloy 2	0.25	0.45	0.15	0.4	Rest.

After the production of Alloy 2 at different sintering temperatures, the microstructure characterization was carried out by optical (Nikon ECLIPSE L150) microscope. Also, the tensile test was performed at 1 mm/min rate with a tensile tester (SHIMADZU with 50kN capacity). After microstructure characterization and tensile tests of Alloy 2, the optimum sintering temperature was determined as 1400 °C. As a result, Alloy 1 and Alloy 2 were pressed and sintered at 1400 °C for 1 h before carburizing process. The carburizing process was carried out by keeping the samples in a sodium cyanide salt bath containing 0.8 C at 925 °C for 4 hr and then cooled in oil bath (oil temperature: 70 °C). Finally, all carburized samples were tempered at 200 °C for 2 hr. Figure 1 gives the images of produced specimens.

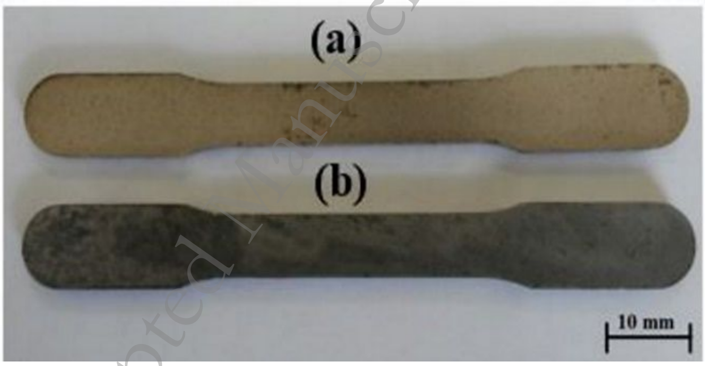

Fig. 1. The image of tensile specimens for Alloy2 that sintered at 1400 °C for 1 h; (a) before carburizing process and (b) after carburizing process.

The produced specimens were subjected to tensile and hardness tests. The densities of the specimens were also measured. Actual densities of the specimens were measured by Archimedes principle. The hardness measurement were performed by using a hardness device (MCT-W, Shimadzu). In order to determine hardness value of the samples, 5 measurements were taken and average value of the measurements was used. The cross section view of the samples was investigated by scanning electron microscope (SEM) (Carl Zeiss Ultra Pluss).

After surface grinding by using 1000 mesh grinding paper, reciprocating wear tests were applied to samples with Tribometer tester (UTS T10/T20). AISI 52100 material steel ball was used for wear test and the stroke distance was kept as 10 mm. The total distance is 1000 meters. Applied load are 15 N and 30 N, and sliding speed is 72 mm/sec. After each wear test the material was cleaned with ethanol and wear weight loss was calculated by electrobalance with 0.1 mg precision. Depth of wear, friction coefficient and friction force were calculated with a software program of the device. Worn surfaces of the samples were then examined by SEM.

3. Results and discussion

3.1. Microstructure characterization and density results

Figure 2 illustrates the microstructures and distribution of grain size of the Alloy-2 that sintered at different temperatures before carburizing process. The grain size of the samples was calculated as 53.1, 43.0 and 95.0 µm, for sintering temperature of 1300 ºC, 1400 ºC and 1500 ºC, respectively. It is observed that grain size of the Alloy 2 has close values at the sintering temperature of 1300 ºC and 1400 ºC. The higher grain size of Alloy 2 at sintering temperature of 1300 ºC can be related to the insufficient sintering which leads to higher porosity [20]. However, increasing sintering temperature from 1400 ºC to 1500 ºC leads to significant grain growth. It is concluded that the optimum sintering temperature (lowest grain size) was determined as 1400 ºC. The grain growth of Alloy 2 at sintering temperature of 1500 ºC can be explained with following reasons. It is known that increasing temperature give rise to accelerate the diffusion of atoms. Fine grains generally prone to grow and combine with increasing sintering temperature. As a result, larger grains can be observed with increasing temperature [21]. It is also reported that grain growth is proportional to the sintering time and temperature [22].

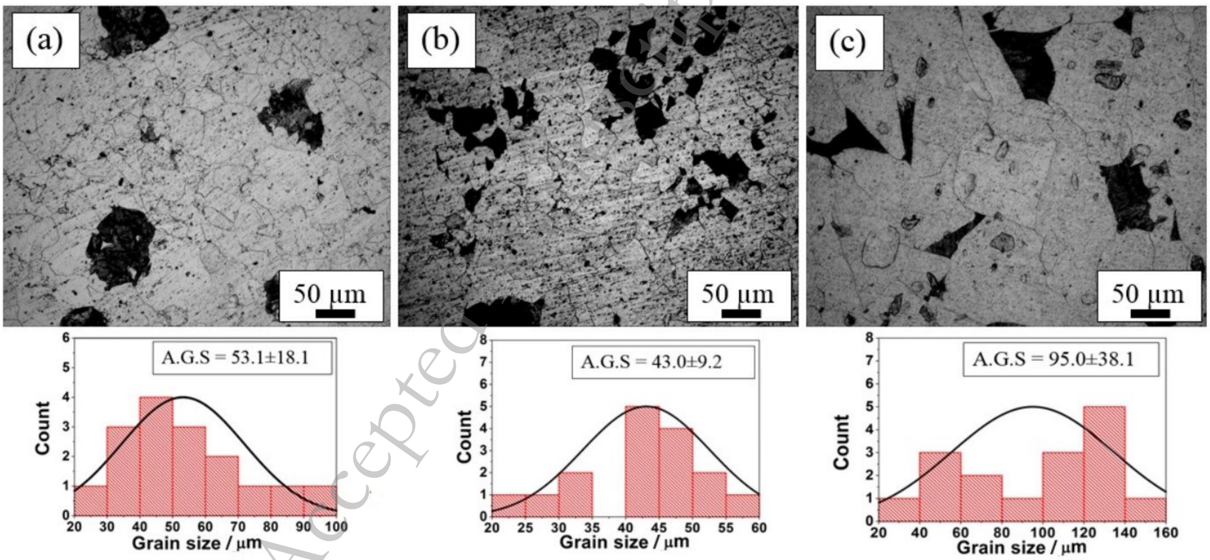

Fig. 2. OM images and grain size distribution of the samples that sintered at different temperatures before carburization (Alloy-2); (a)1300 ºC, (b)1400 ºC and (c)1500 ºC.

Figure 3 shows the microstructure of uncarburized and carburized condition for Alloy-2. It is clear that the microstructure consists of ferrite and pearlite phases (Fig.3a). It is seen that carbon layer on the surface was observed after carburizing (Fig.3b). As can be seen in Fig. 3b, dark layer is the carbon layer at the outer surface of sample.

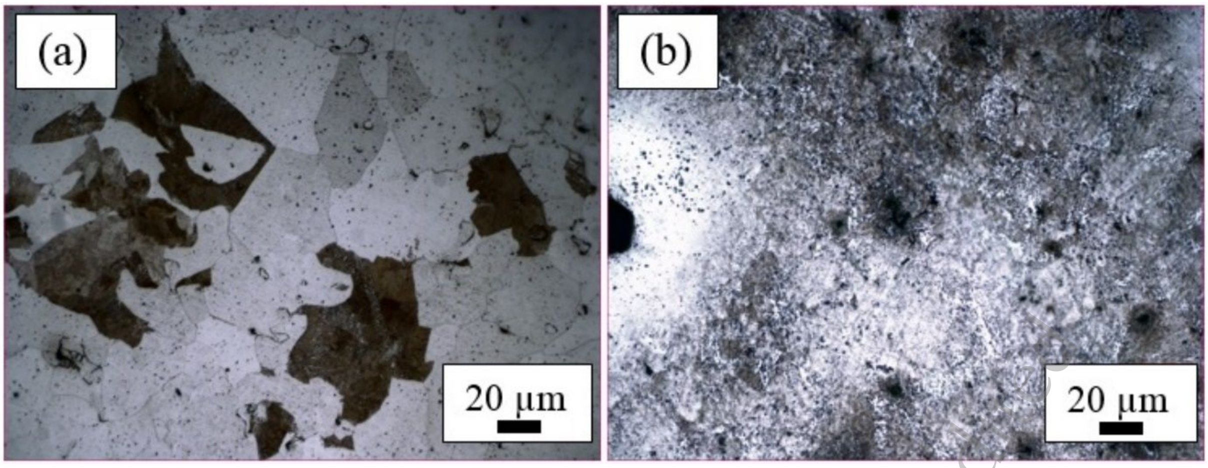

Fig. 3. The OM images of Alloy-2 that sintered at 1400ºC (a) un-carburized and (b) carburized conditions.

The density values of the Alloys were given in Table 3. It is seen that relative density of alloys increased after sintering process when compared to non-sintered conditions (green density). The green density of Alloy 1 and Alloy 2 was measured as 6.745 g/cm^3 and 6.819 g/cm^3, respectively. However, sintered density of Alloy 1 and Alloy 2 was reported as 6.945 g/cm^3 and 6.948 g/cm^3, respectively. It is concluded that sintering process caused an increase in relative density and a decrease in porosity. The reason of sintered density is higher than green density is that the sintering process allows diffusion of atoms and reduces porosity of alloys [22]. It is also worth to say that carburizing treatment leads to slight increase in relative density compared to non-carburized conditions. Similar studies agree that sintering process increases the relative density of the samples [23,24].

Table 3. Density results of the Alloy

Treatment	Alloy 1					Alloy 2				
	Green density / (g.cm^{-3})	Relative density (Before Sintering %)	Sintered density / (g.cm^{-3})	Relative density (After sintering %)	Porosity / %	Green density / (g.cm^{-3})	Relative density (Before Sintering %)	Sintered density / (g.cm^{-3})	Relative density (After Sintering %)	Porosity / %
Pre-carburizing	6.745	87.59	6.945	90.11	9.89	6.819	88.55	6.948	90.17	9.83
After-carburizing	-	-	7.036	90.66	9.34	-	-	7.037	91.32	8.68

The dispersion of carbon layer of the samples was shown in Fig.4. The average thickness of the carburized layer was calculated for Alloy 1 and Alloy 2 as 29.68 μm and 42.99, respectively. It is well known that processing temperature and time are the most important parameters for carburizing. The thickness of carburized layer increases with increasing carburizing temperature and carburizing time [14]. It is also reported that substrate material has an important effect on kinetics of carburizing process. Sun has investigated the kinetics of carburizing of different steels and concluded that steel with high Mo content has higher layer thickness. This situation is associated with higher carbon transfer at the surface and higher carbon diffusion rate of the layer [25]. For this study, the carburizing process was performed at constant condition for both alloys (925 °C -4 hr). The higher carburizing thickness of Alloy 2 can be related to the presence of more free carbon in the structure which facilitates the diffusion [25].

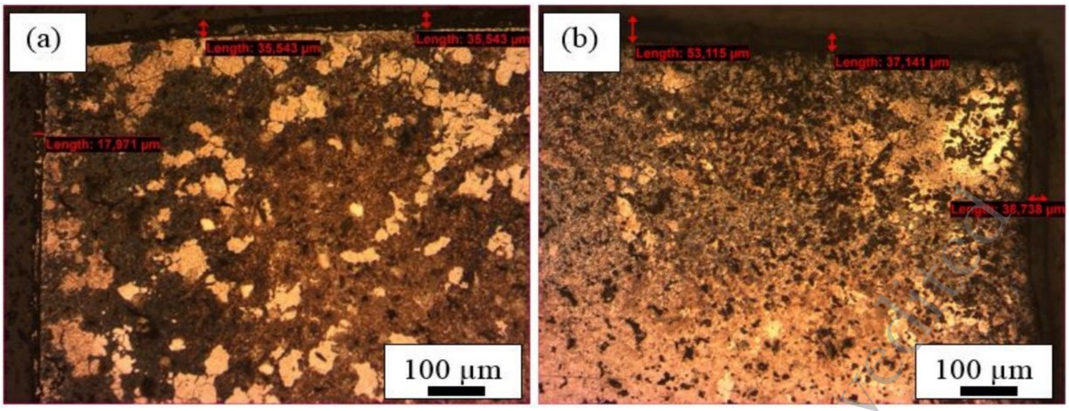

Fig. 4. Cross section view of the samples a) Alloy 1 and b) Alloy 2

Figure 5 shows EDS analysis of carburized Alloy-2. It is clear from the Fig 5.a, the significant amount of C was detected for the analysis of all points. The EDS line analysis in Fig. 5b shows that amount of carbon element in carburized AISI 8620 PM steel vary along the line intersecting the matrix. It is determined that matrix phase is rich in iron however, carbon layer is rich in coating. It is seen that there is acute increase in amount of carbon at the intersection of analysis line with carburizing treatment. It is concluded that carburizing leads to formation of carbon layer on the surface.

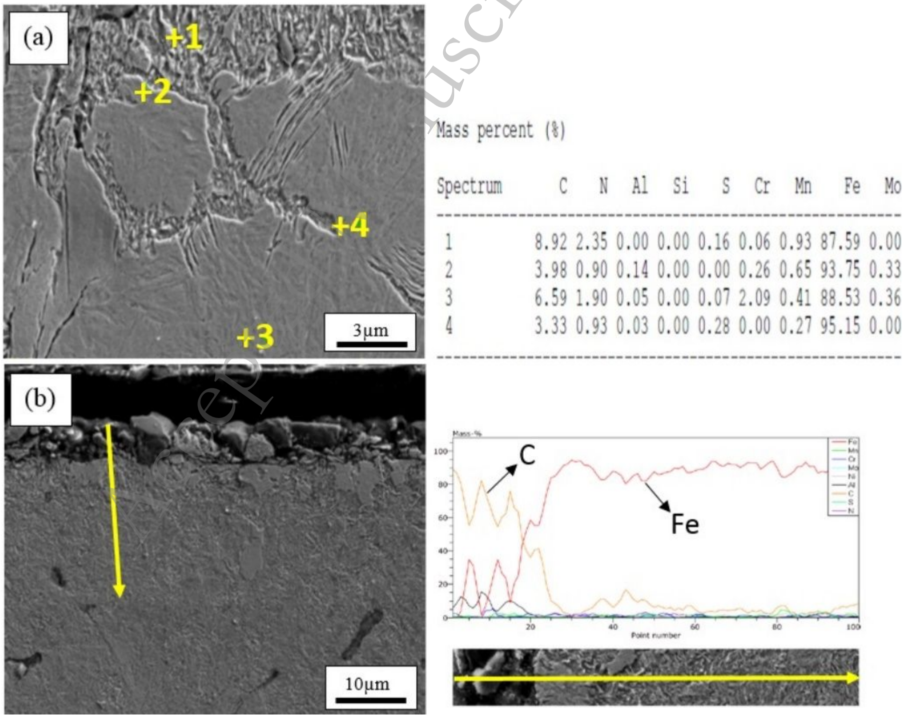

Spectrum	C	N	Al	Si	S	Cr	Mn	Fe	Mo
1	8.92	2.35	0.00	0.00	0.16	0.06	0.93	87.59	0.00
2	3.98	0.90	0.14	0.00	0.00	0.26	0.65	93.75	0.33
3	6.59	1.90	0.05	0.00	0.07	2.09	0.41	88.53	0.36
4	3.33	0.93	0.03	0.00	0.28	0.00	0.27	95.15	0.00

Fig. 5. The EDS analyses of the Alloy-2 a) micrograph and b) cross section view

3.2. Mechanical properties

Figure 6 displays the diagram of stress-strain for Alloy-1 and Alloy-2. The hardness and tensile test results are also given in Table 4. It can be noted that the mechanical properties of the Alloys increased with increasing sintering temperature from 1300°C to 1400°C. However, the sintering temperature of more than 1400 °C, give rise to decrease in mechanical properties of both Alloys. For example, ultimate tensile strength of Alloy 2 decreased from 261.2 MPa to 215.7 MPa when sintering temperature changed from 1400 °C to 1500 °C. As a result, it is concluded that the highest hardness and mechanical properties for both alloys were obtained at sintering temperature of 1400 °C. The low hardness and mechanical properties of both alloys at sintering temperature of 1300 °C can be attributed to the insufficient sintering. It is reported that insufficient sintering leads to formation of high porosity, decrease in mechanical properties [20]. The higher mechanical properties of Alloys at sintering temperature of 1400 °C can be explained with Hall-Petch equation. This relationship suggests that higher strength is expected in materials having smaller grain size [26]. For this study, this situation was supported with microstructure images for Alloy 2 (Fig. 2). The grain size of Alloy 2 at sintering temperature of 1300°C, 1400°C and 1500 °C was calculated as 53.1, 43.0 and 95.0, respectively. However, at sintering temperature of 1500 °C, the hardness and mechanical properties decreased significantly due to grain growth.

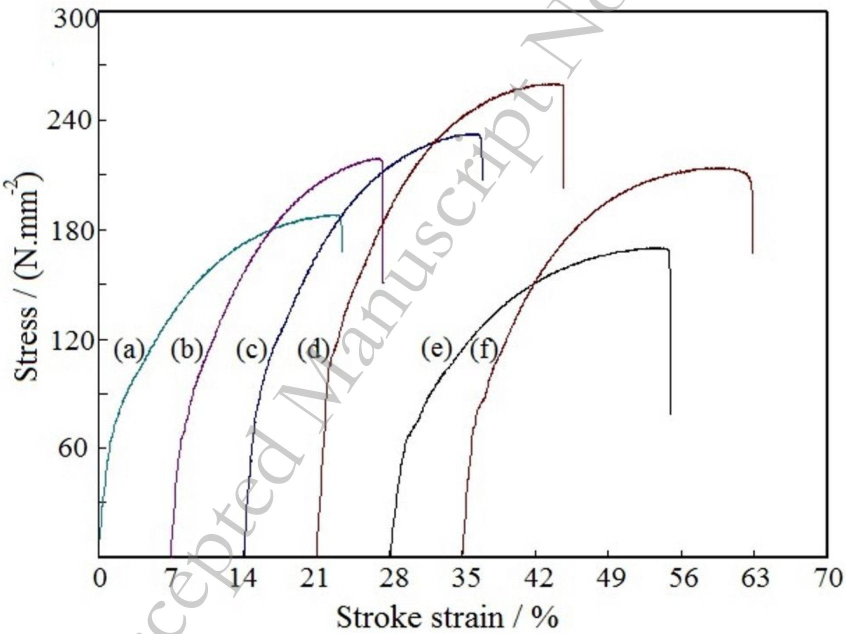

Fig. 6. Variation of stress-strain curves for different sintering temperatures; 1300°C a) Alloy 1, b) Alloy 2; 1400°C c) Alloy 1, d) Alloy 2 and 1500 °C e) Alloy 1, f) Alloy 2

Table 4. Hardness and tensile test results of the Alloy-1 and Alloy-2

Sintering Temperatures /°C	Alloy 1				Alloy 2			
	YS / MPa	UTS / MPa	E / %	Hardness / $HV_{0.5}$	YS / MPa	UTS / MPa	E / %	Hardness / $HV_{0.5}$
1300	75.8	188.6	22.3	100.4±2.1	93.2	220.3	19.9	106.1±2.1
1400	97.4	234.3	21.7	105.6±2.9	105.4	261.2	22.4	113.7±3.4
1500	69.3	215.7	24.3	97.3±3.1	88.1	215.7	24.3	101.4±1.9

Figure 7 displays the tensile strength of the samples for carburized and un-carburized conditions. It can be seen that carburizing give rise to enhancement of tensile strength owing to the formation of carbon layer on the surface. Eghbali et al. also reported that there is an important relation between microstructures and stress-strain responses during deformation by higher carburizing process [27]. Lou et al. also showed that the process time and temperature significantly affected the mechanical properties [28].

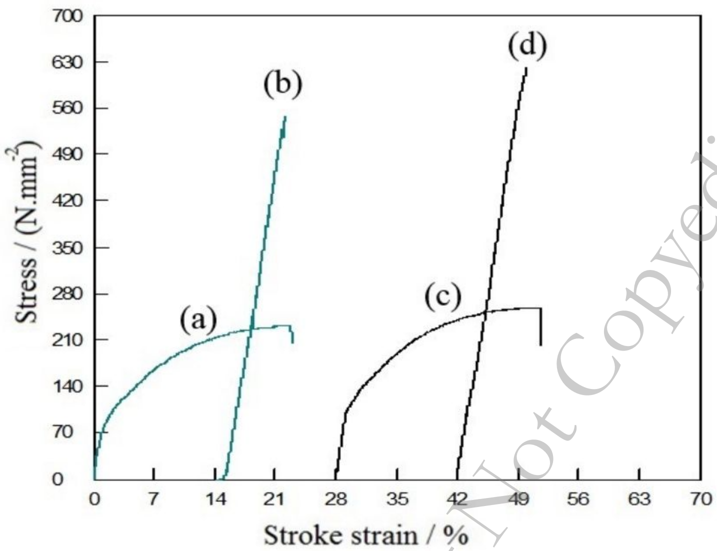

Fig. 7. Variation of stress–strain curves of the samples (a) pre-carburizing Alloy-1, (b) after-carburizing Alloy-1, (c) pre-carburizing Alloy-2 and d) after-carburizing Alloy-2

Table 5 also shows the tensile test and hardness values of un-carburized and carburized samples. It can be seen that carburizing give rise to significant effect on hardness and mechanical properties. The hardness of un-carburized Alloy-2 is 113.7 HV. When the carburized treatment applied the sample, the hardness value increase from 113.7 to 401.3 HV. It is known that the heat facilitates the diffusion of C atoms to surface with increasing temperature. As a result, the higher hardness was obtained [28]. Luo et al. [29] also have reported that after carburization, considerable increase in hardness was observed. Carburization also contributes to increase the strength via the precipitation such as CrC formed during sintering after slow cooling and carburization treatment. Erden [30] showed that after sintering and cooling, VC(N) or NbC(N) precipitates form during the austenite-ferrite transformation of microalloyed steels. This precipitates lead to increase in strength values. It is well known that density also affects the mechanical properties because the voids formed by sintering decrease the strength, heat transfer and cooling rate of the material. It is well known that formability and toughness depends on density [31].

Table 5. Mechanical properties of carburized alloys.

Alloy	Yield Strength / MPa	Ultimate Tensile Strength / MPa	Elongation / %	Hardness / HV0.5
Pre carburizing Alloy-1	92.1	234.3	21.7	95.1±2.1
Pre carburizing Alloy-2	105.7	261.7	22.4	113.7±3.4
After carburizing Alloy-1	290.9	549.4	8.1	375.2±3.9
After carburizing Alloy-2	305.3	623.2	7.9	401.3±4.5

3.2.1. Fracture surface examination

Figure 8 shows the fracture surface images of Alloy-1 and Alloy-2 that sintered at different temperatures. It can be observed that several dimples are present on the fracture surface for both alloy at sintering temperature of 1300 °C. The presence of dimples is the evidence of ductile failure mode. The ductile fracture is also explained by the occurance of microvoid coalescence, which leads to presence of larger sized dimples [24]. However, cleavage planes are clearly discernible for the fracture surface of Alloy-2 sintered at 1500 °C. The presence of dimples and cleavage facets indicates that fracture mode is ductile and brittle [23]. The low mechanical properties of Alloys at sintering temperature of 1300 °C can be attributed to the presence of high angular porosity which leads to stress concentration. As a result, crack initiation and poor load bearing capacity are observed [32]. The large voids are also seen for the fracture surface of Alloys at 1400 °C. This situation is explained by detaching the some carbides during tensile tests [33]. It is also worth to say that the transition from ductile to brittle fracture is present with increasing sintering temperature. The same observation was reported for different study about sintering behaviour of Fe-P alloys [23].

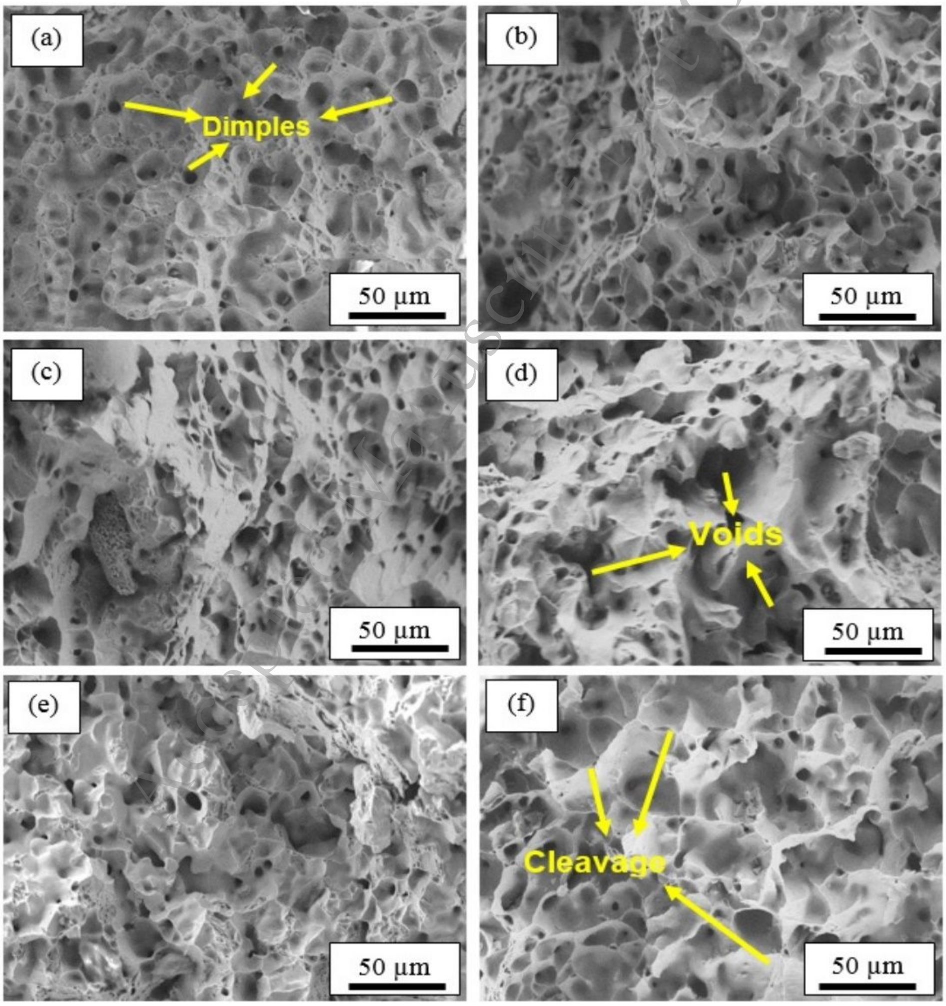

Fig. 8. SEM fractographs of (a) Alloy-1 (b) Alloy-2 sintered at 1300 °C, (c) Alloy-1 (d) Alloy-2 sintered 1400°C , (e) Alloy-1 (f) Alloy-2 sintered at 1500°C.

3.3. Wear Test Results

Figure 9 displays the variation of wear depth of the samples depending on sliding distance. At load of 15N, wear depth values of the samples is minimum and at load of 30N wear depth has maximum value. It can be said that wear depth increases with increasing applied load. Uncarburized samples showed higher wear depth, while carburised samples revealed the minimum wear depth due to their higher hardness. Also, it can be seen that Alloy-2 exhibits the best wear performance under all conditions.

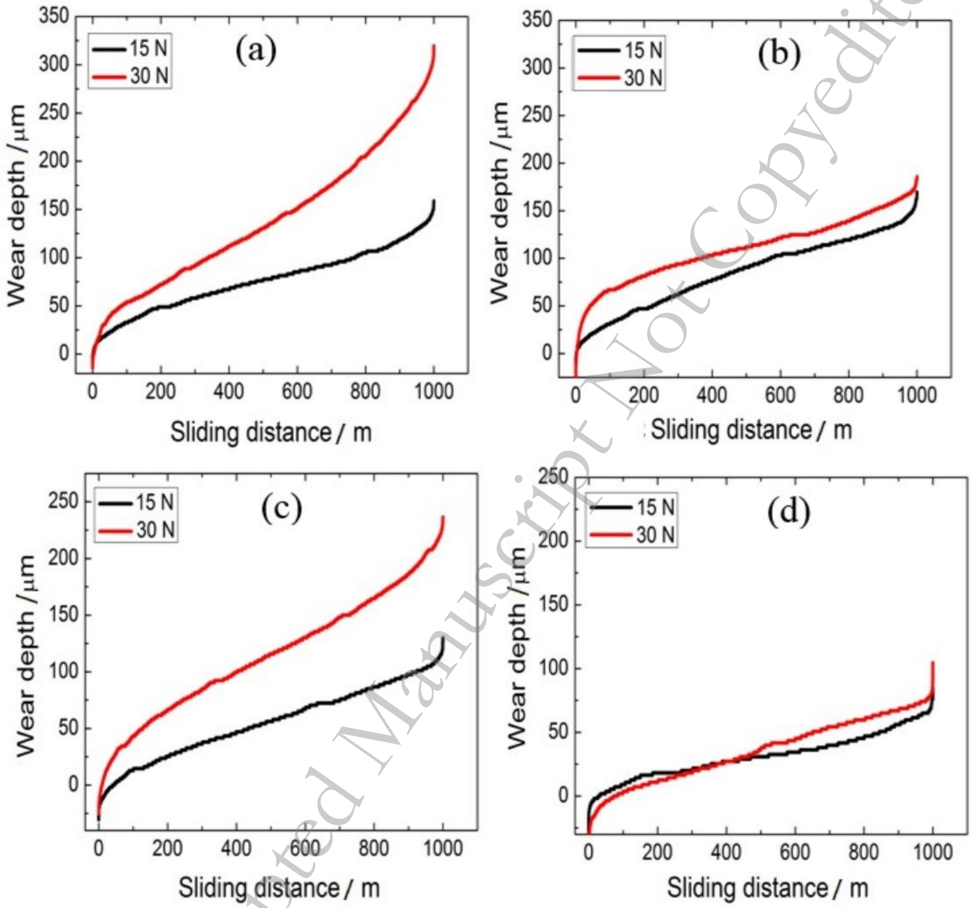

Fig. 9. Wear depth graphs of the samples for Alloy-1; a) pre-carburizing, b) after-carburizing, for Alloy-2 c) pre-carburizing and d)after-carburizing.

The wear test results of the samples were given in Table 5. It is clear that the average coefficient of friction decreased with increasing load for all samples. The carburizing treatment give rise to decrease in average coefficient of friction for the samples for all conditions. The weight loss and wear depths of the all samples shows significant enhancement in comparison with un-carburized condition. Alloy-2 with carburized condition exhibits the best wear performance. Singh et al. [34] studied heat treatments such as quenching, carburizing and tempering. After the carburizing and tempering, mild steels are subjected to wear, hardness and tensile test. It is reported that wear resistance increases with increasing soaking time. Emamian studied the effect of solid carburization on mechanical and tribological performance of powder metallurgy parts. The effects of austenitization and quenching are investigated and concluded that wear resistance can be increased with moderate hardness [17].

Table 6. Wear test results of the samples.

Treatment	Load / N	Weight Lost / g	Wear Depth / μm	Average Coefficient of Friction
Pre Carburizing	15	0.0012	155.3	0.69
(Alloy-1)	30	0.0091	323.3	0.63
After Carburizing	15	0.0003	152.1	0.55
(Alloy-1)	30	0.0008	175.2	0.46
Pre Carburizing	15	0.0009	118.7	0.65
(Alloy-2)	30	0.0076	231.2	0.61
After Carburizing	15	0.0002	68.2	0.57
(Alloy-2)	30	0.0003	100.1	0.49

3.3.1. Worn surface analysis

Figure 10 indicates the worn surface images of the samples. It is seen that compact oxide layers (black areas) are present on the worn surface of Alloy 1 under load of 15 N. However, the area of oxide layer increased for Alloy 2 under same load. It can be said that partly oxidative wear is present for both of Alloy 1 and Alloy 2 under load of 15 N. The oxidation is the result of frictional heating during sliding [35]. It is known that higher load leads to higher frictional heating and higher surface temperature. This causes higher chemical reactivity of surface and rapid growth of oxide film. However, it is reported that higher stress occurs with increasing load. As a result, the higher stress on the surface give rise to severe mechanical deformation, which restrains the formation and growth of oxide film on the worn surface [36,37]. It can be observed that grooves are parallel to the sliding direction. This verifies the presence of abrasion [38-40]. For Alloy 2, grooves changed to fine scratches under load of 30 N. It is concluded that wear mechanism is mild abrasive. Also, from the transition load of 15 N to load of 30 N, oxidative wear changed to abrasive wear for all samples. Figure 11 shows the EDS analysis of Alloy 2 under load of 15 N. In order to clarify the chemical composition, EDS analysis was applied for different areas. The EDS analysis of point 1 shows significant amount of Fe (92.75%) and low amount of O (4.66%). However, the EDS analysis of dark area (point 4) verifies the presence of high amount of O (32.44%). From the EDS analysis, it can be concluded that dark areas belong to oxidation areas.

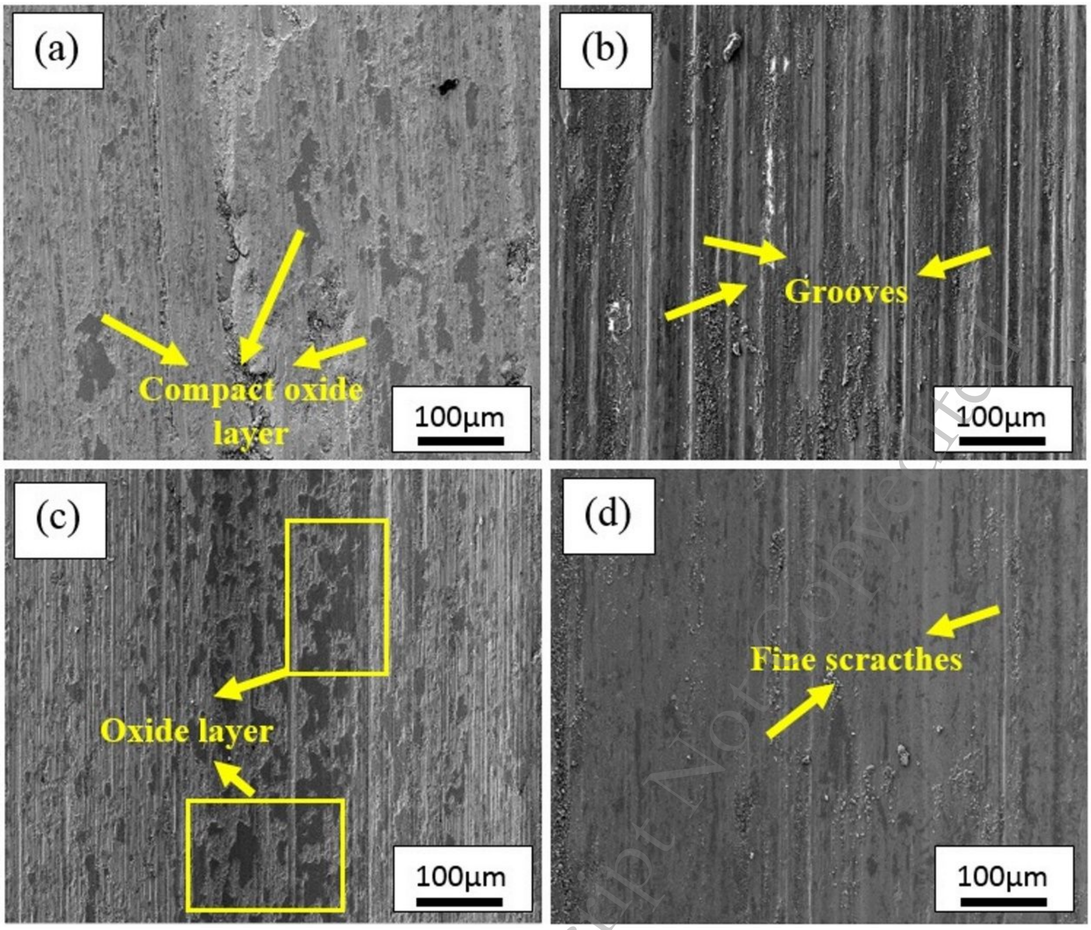

Fig. 10. The worn surface images of the samples a) Alloy 1 (load of 15N) b) Alloy 1 (load of 30N), c) Alloy 2 (load of 15N) and d) Alloy2 (load of 30N)

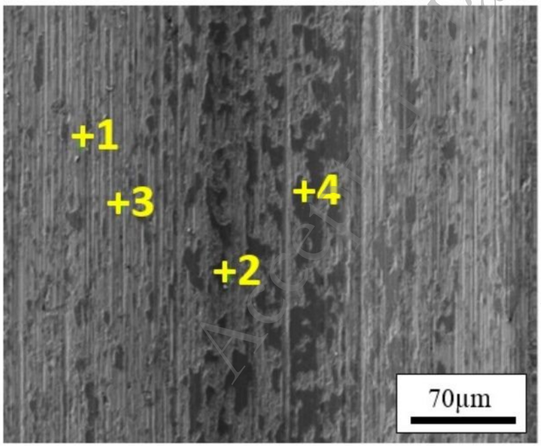

Mass percent (%)

Spectrum	C	O	Si	P	S	Cr	Mn	Fe	Co	Ni
1	0.00	4.66	0.15	0.09	0.07	0.22	2.06	92.75	0.00	0.00
2	0.00	1.04	0.07	0.04	0.10	1.12	2.23	95.38	0.00	0.00
3	2.28	12.02	0.53	0.00	0.00	0.62	0.19	83.42	0.56	0.38
4	1.54	32.44	0.08	0.00	0.02	0.50	0.19	64.41	0.71	0.09

Fig. 11. The EDS analysis of Alloy 2 under load of 15 N.

4. Conclusions

In this study, AISI 8620 steels are successfully produced by powder metallurgy and carburized at 925 °C for 4 hr. The following results were obtained for this study.

- The average thickness of the carburized layer was calculated for Alloy 1 and Alloy 2 as 29.68 µm and 42.99, respectively.
- The carburizing treatment give rise to significant increase in hardness and tensile strength in comparison with uncarburized specimens. This is related to the presence of hard carburization layer.
- The wear resistance of carburized alloys is higher than that of uncarburized alloys. Also, average friction coefficient tend to decrease with carburization process. The worn surface analyses show that oxidative wear is present under load of 15 N. However, oxidative wear changed to abrasive wear for higher load.

References

[1] S. Wan, H. Li, K. Tieu, Q. Xue and H Zhu, Mechanical and tribological assessments of high-vanadium high-speed steel by the conventional powder metallurgy process, *Int J Adv Manuf Tech.,* 103 (2019), p. 943.

[2] S. Gündüz, M.A. Erden, H. Karabulut and M. Türkmen, Effect of vanadium addition on the microstructure and mechanical properties of low carbon micro-alloyed powder metallurgy steels, *Mater. Test.,* 55 (2016) No. 4, p. 433.

[3] W Shen, L Yu, H Liu, Y He, Z Zhou and Q Zhang, Diffusion welding of powder metallurgy high speed steel by spark plasma sintering, *J Mater. Process. Technol.,* 275 (2020) p. 1.

[4] M.A. Erden, Effect of pressing pressure on microstructure and mechanical properties of non-alloyed steels produced by powder metallurgy method, *OHU J. Eng. Sci*., 6 (2017), No 1, p. 257.

[5] D. Sivaprahasam, S.B. Chandrasekhar, K. Murugan and K.V.P. Prabhakar, Microstructure and mechanical properties of M62 high-speed steel powder consolidated by high temperature gas extrusion, *Mater. Res. Innov*., 24 (2020), No. 1, p. 52.

[6] B. Pekgöz, S. Saridemir, İ. Uygur and Y. Aslan, The effects of carburisation process on the hardness values and microstructure for steels, *Electronic J Machine Technologies*, 10, (2013), No. 1, p. 19.

[7] S. Roy and S. Sundararajan, The effect of heat treatment routes on the retained austenite and tribomechanical properties of carburized AISI 8620 steel, *Surf. Coat. Technol.,* 308, (2016), p. 236.

[8] M. Izciler and M. Tabur, Abrasive wear behavior of different case depth gas carburized AISI 8620 gear steel, *Wear,* 260 (2006) p. 90.

[9] M. Erdogan and S. Tekeli, The effect of martensite particle size on tensile fracture of surface-carburised AISI 8620 steel with dual phase core microstructure, *Mater. Des.*, 23(2002), No. 7, p. 597.

[10] Y.Y. Özbek, M. Durman and H. Akbulut, Wear Behavior of AISI 8620 steel modified by a pulse-plasma technique, *Tribol. T.* 52(2009), No.2, p. 213.

[11] S. Patidar, A. Jain and D Singh, Effect of tempering temperature and applied load on various wear environment of carburized mild steel, *IOSR-JMCE*, 3(2012), No. 3,p.62.

[12] M. Kumar and R.C. Gupta, Abrasive wear characteristics of carbon and low alloy steels for better performance of farm implements, *J. Mater. Sci. Technol.*, 11 (1995), p. 91.

[13] R.R. Panda, A.M Mohanty and D.K Mohanta, Mechanical and wear properties of carburized low carbon steel samples, *IJMCR*, 2(2014), p. 109.

[14] M.A. Abdulrazzaq, Investigation the mechanical properties of carburized low carbon steel, *Int. J. Eng. Res. Appl.,* 6(2016), No.9, p. 59.

[15] H. Elzanaty, Effect of carburization on the mechanical properties of the mild steel, *IJIAS*, 6 (2014), No. 4, p. 987.

[16] S. Chauhan, V. Verma, U. Prakash, P.C. Tewari and D. Khanduja, Analysis of powder metallurgy process parameters for mechanical properties of sintered Fe–Cr–Mo alloy steel, *Mater. Manuf. Process.* 32(2017), No. 5, p. 537.

[17] A. Emamian, A study on wear resistance, hardness and impact behaviour of carburized Fe-based powder metallurgy parts for automotive applications, MSA, 3 (2012), p. 519.

[18] X. Dong, J. Hu, H. Wang, S. Liu and Z. Guo, A study on carbon concentration distribution and microstructure of P/M materials prepared by carbusintering, *J. Mater. Process. Technol.* 209 (2009), p. 3776.

[19] J. Georgieva, T. Pieczonkab, M. Stoytcheva and D. Teodosievc, Wear resistance improvement of sintered structural parts by C_7H_7 surface carburizing, *Surf. Coat. Technol*. 180–181 (2004), p.90.

[20] N. Kurgan, Effect of porosity and density on the mechanical and microstructural properties of sintered 316L stainless steel implant materials, *Mater. Des.* 55 (2014), p. 235.

[21] M.A. Erden, The effect of the sintering temperature and addition of niobium and vanadium on the microstructure and mechanical properties of microalloyed PM steels, *Metals. 7,* (2017), No. 9, p. 329.

[22] M. Rahimian, N. Parvin and N. Ehsani, The effect of production parameters on microstructure and wear resistance of powder metallurgy Al–Al_2O_3 composite, *Mater. Des.* 32 (2011), p. 1031.

[23] A. Muthuchamy, R. Kumar, A.R. Annamalai, D.K. Agrawali and A. Upadhaya, An investigation on effect of heating mode and temperature on sintering of Fe-P alloys, *Mater. Charact.* 114 (2016), p.122.

[24] M.A Erden, S. Gündüz, M. Türkmen and H. Karabulut, Microstructural characterization and mechanical properties of microalloyed powder metallurgy steels, *Mater. Sci. Eng. A* 616 (2014), p. 201.

[25] Y. Sun, Kinetics of low temperature plasma carburizing of austenitic stainless steels, *J. Mater. Process. Technol.* 168 (2005), p. 189.

[26] M. Rahimian, N. Ehsani, N. Parvin and HR Baharvandi, The effect of particle size, sintering temperature and sintering time on the properties of Al–Al2O3 composites made by powder metallurgy, *J. Mater. Process. Technol.* 209 (2009), p. 5387.

[27] B. Eghbali, A. Abdollah-Zadeh, H. Beladi and P.D. Hodgson, Characterization on ferrite microstructure evolution during large strain warm torsion testing of plain low carbon steel, *Mater. Sci. Eng. A,* 435-436(2006), p. 499.

[28] D.C. Lou, J.K. Solberg and T. Børvik. Surface strengthening using a self-protective diffusion paste and its application for ballistic protection of steel plates, *Mater Des.* 30 (2009), No. 9, p. 3525.

[29] Y. Luo, H. Jiang, G. Cheng and H. Liu, Effect of carburization on the mechanical properties of biomedical grade titanium alloys, *J Bionic Eng,* 8(2011), p. 86.

[30] M.A. Erden, Effect of C content on microstructure and mechanical properties of Nb-V added microalloyed steel produced by powder metallurgy method, *EJST*. 5 (2016), No. 9, p. 44.

[31] D.R. Askeland, P.P. Fulay and W.J. Wright, The science and engineering of materials, 1st ed.; Chapman and Hall: London, UK, 1996.

[32] S. Pandya, K.S.Ramakrishna, A.R. Annamalai and A. Upadhyaya, Effect of sintering temperature on the mechanical and electrochemical properties of austenitic stainless steel, *Mater. Sci. Eng. A,* 556 (2012), p. 271.

[33] D Shanmugasundaram and R. Chandramouli, Tensile and impact behaviour of sinter-forged Cr, Ni and Mo alloyed PM steels. *Mater. Des.* 30 (2009), No.9, p. 3444.

[34] S. Singh, D. Singh, K. Sachan and A. Arya. Effect of soaking time and applied load on wear behavior of carburized mild steel, *IOSRJEN*, 3(2013), No.2, p.10.

[35] C.Y.H. Lim, S.C. Lim and M. Gupta, Wear behaviour of SiCp-reinforced magnesium matrix composites, *Wear*, 255 (2003), No. 6, p. 629.

[36] F.Labib, H.M. Ghasemi and R.Mahmudi, Dry tribological behavior of Mg/SiCp composites at room and elevated temperatures, *Wear,* 348-349 (2016), p. 69.

[37] F. Aydin, Y. Sun, H Ahlatci and Y. Turen, Investigation of microstructure, mechanical and wear behaviour of B_4C particulate reinforced magnesium matrix composites by powder metallurgy. *Trans Indian Inst Met*. 71(2018), p.873.

[38] F. Aydin and Y. Sun, Investigation of wear behaviour and microstructure of hot-pressed TiB_2 particulate-reinforced magnesium matrix composites, *Can. Metall. Quart.* 57 (2018), No. 4, p. 455.

[39] F. Aydin and, Y. Sun, Microstructure and wear of a sintered composite with a magnesium alloy AZ91 matrix reinforced with ZrO_2 particles. *Met. Sci. Heat. Treat.* 61 (2019), p. 325.

[40] F. Aydin , Y. Sun and M.E. Turan, Influence of TiC content on mechanical, wear and corrosion properties of hot-pressed AZ91/TiC composites, *J Compos. Mater.* 54 (2020), No. 2, p.141.